Scientific Journals
of the Maritime University of Szczecin

Zeszyty Naukowe
Akademii Morskiej w Szczecinie

2023, 74 (146), 5–15
ISSN 2392-0378 (Online)
DOI: 10.17402/559

Received: *14.11.2022*
Accepted: *28.02.2023*
Published: *30.06.2023*

Handling and transportation properties of rapeseed biomass as affected by particle size

Milena Bojanowska

https://orcid.org/0000-0003-0149-2281

Maritime University of Szczecin, Faculty of Economics and Transport Engineering
11 Henryka Pobożnego St., 70-507 Szczecin, Poland
e-mail: m.bojanowska@pm.szczecin.pl

Keywords: rapeseed meal, rapeseed cake, canola, biomass, agricultural commodities, bulk storage, flowability, logistics vulnerability, particle size, angle of repose, porosity, bulk density, agricultural bulk solids

JEL Classification: R41, Q42, Q170

Abstract

Rapeseed by-products of seeds de-oiling, particularly expellers and post-extracted meal, are currently considered an important biomass that can be used as an alternative energy source, either in raw form or after conversion to biochar. Rapeseed biomass represents a difficult-to-handle cargo, mainly due to its sensitivity to mechanical, climatic, and biological impacts, as well as its dusty nature. This study aims to determine the physical properties of rapeseed meals and their fractions. Morphological and chemical features of six particle sets are investigated in order to explain the variation in their physical properties having importance in handling and transportation processes. The true density of fractions increases when the particle size decreases due to the diminishing quantitative share of seed coats. No correlation is observed between true and bulk densities, as the particle shape, surface sculpture, and adhesion affect the mutual particle arrangements. Along with a decrease in the particle size from 0.4 mm, a rapid decrease in the flowability is observed. The tendency of the finest dust (d < 0.075 mm) to form agglomerated complexes causes its lower bulk density, higher porosity, and higher angles of repose in comparison to coarse dust (0.075–0.4 mm). It is concluded that a relatively low tendency to free flowing of natural RSM is mainly caused by its wide-ranging particle size distribution and their geometry differentiation, which facilitate mutual particle interlockings. The known cases of blockages of silos, bins, hoppers, and transfer chutes may be mainly caused by the powder fractions (< 0.2 mm), with a much lower flowability than other particles.

Introduction

Rapeseed (*Brassica napus* L.), with an annual global output reaching 73.8 million tons, is a crop that is currently of the second greatest importance after soybean in the vegetable oil industry (USDA, 2022). Expellers and post-extracted meals, frequently termed by the common name "oilseed cake", constitute by-products in oil production. Global production of rapeseed meal (RSM) reached 41.8 million tons in the 2020/2021 season, which accounted for a 12% share of the total supply of oily meals. Poland is one of the leading producers of rapeseed and its products in UE, including RSM, alternatively used as feedstuff or solid biofuel in green energy production. Export of RSM from Poland, largely carried out by sea, exceeds 50% of the production volume in the last 10 years, reaching the level of 600–700 thousand tons per year (Fediol, 2021).

For the large-volume deliveries of RSM by land in Poland, railway transport is dominant, while road carriages play a secondary role. RSM biomass delivered to seaports is transported in Tadds, Ugpps, Tads, and Tadgns wagons. The unloading of silos at production plants, as well as railway wagons and self-dumping trucks or tanks for solid materials, is gravitational through the use of self-unloading bottom structures, while some types of transport means are loaded using pneumatic loading devices. The technology of rapeseed biomass transportation processes includes conveyor systems besides the usual gravity loading, which is associated with the problems of self-sorting, dusting, and deposition of fine particles on the surfaces of devices and means of transport. The common use of central dust aspiration systems, as well as individual filters installed in places of particular dusting, significantly reduces the formation of dust-air mixtures during operations, but it does not solve the problems of RSM self-sorting and accumulation of settled dust.

In former studies, it was presented that RSM is highly dusting and features large dispersion of particle size (Fauduet et al., 1995). The proportion of dusty fractions (d < 0.4 mm) of RSM in domestic production reaches 25% (m/m). In an average weight of 5 thousand tons of rapeseed meal cargo handled in the warehouse-ship relation, about 5 tons of the finest dust with a particle size of d < 0.075 mm (0.1% m/m) and 270 tons of dust with granulation of 0.075–0.2 mm (5.8% m/m) were moved (Bojanowska, Chmiel & Pańcyk, 2016). The presence of powdery fractions in plant-origin materials is considered undesirable during storage, handling, and transportation due to the creation of a dense structure by filling free spaces in the already-formed layer, causing more ventilation difficulties (Horabik, 2001). Finest fractions may also be the reason for material stream blockages during unloading due to the inter-particle and boundary cohesion and adhesion forces (Carr, Roberts & Wheeler, 2019). Self-sorting of RSM during the handling processes causes, in the storage and transportation facilities, a settlement solely of the finest dust in practice. Rapeseed dust deposits on machinery accelerate mechanical wear and lead to erosion, pose a risk of explosion (Bojanowska, Chmiel & Pańcyk, 2016), and enhance self-heating processes (Sturaro et al., 2003).

Fine dust particles of rapeseed biomass are also burdensome in transportation and storage processes due to the different chemical composition compared to coarse-grained fractions. Three types of morphologically and chemically varied particles can be distinguished in RSM: cotyledon residues, seed coat scraps, and their agglomerates. Mechanical resistance of rapeseed coat causes the phenomenon of the finest dust formation in RSM exclusively from the cotyledons (Sosulski & Zadernowski, 1981; Mińkowski, 2002). The proportion of seed coat's particles descends with decreasing size of mesh screens – the majority remains on the sieve with a size of 0.4 mm (Bojanowska & Leśmian-Kordas, 2009). This, in turn, implies a different chemical composition of the dust compared to the unfractionated meal: a lower fat and crude fiber but higher protein content (Chibowska, Smulikowska & Pastuszewska, 2000).

Problems with handling rapeseed meal result not only from the presence of dust fraction but also from its low flowability as determined from practice. RSM can be stored in specially adapted silos made of reinforced concrete or metal, which constitutes autonomous structures or chambers that are part of grain elevators, as well as in flat-bottomed warehouses. In industrial practice, storage of seed cakes in metal silos, especially in those that are not adapted to that type of cargo, is avoided. The specialized warehouses built for long-term storage of this particulate type of loads, i.e., post-extracted oily meals or seed expellers, are floor structures with a greater bottom surface compared to the height. This is due to a lower flowability of seed meals in comparison to other cargoes of plant origin and their susceptibility to the phenomenon of "bridging", i.e., the formation of vaultings over the outlets of storage chambers (Koch & Noworyta, 2003). The suspension of granular material during the unloading may result in serious damage, especially when it occurs in silos where a large mass of cargo is stored. There are known cases of such accidents with RSM involved. In 2006, at the production plant in Brzeg (Poland), during the unloading of the reinforced concrete silo filled with RSM, the silo's roof collapsed and the technological line was completely destroyed as a result of a massive implosive accompanying the disturbed flowing of material (PIP, 2006). The primary causes of this accident were processes of agglomeration and compaction of the stored meal. After the first stage of material free flow during unloading, the rest of the agglomerated vast mass of load was suspended, eventually falling in an uncontrolled way and simultaneously creating strong negative pressure in the upper part of the silo. Currently, the largest domestic manufacturers of RSM use, for its short-term storage, silos made of reinforced concrete or metal. However, these constructions are additionally secured by flaps installed in various parts of the structure, which are used to equalize pressure in the case of suspension of material and to prevent the creation of negative pressure in the upper part of the tank.

As current practice shows, the choice of a storage building during the RSM handling in transshipment hubs may be determined, rather than by requirements specified for a certain type of load (especially if they are not covered by regulations), by the logistic needs of the entire terminal in which other cargoes are handled at the same time. In Polish seaports, flat-bottomed warehouses are usually first filled with soybean meal imported by sea for fodder purposes (2.7 mln tons in 2020), which is currently one of the most important agri-bulk cargoes (after grain) in terms of tonnage (Fediol, 2021). Generally, in seaports across the EU, there is a lack of specialized biomass terminals. Despite the increasing volume of transshipments of agricultural and forest biomass, it is still not an attractive cargo for the main hubs, while in the minor ports (regional or medium-sized) it is usually handled at bulk (ore and coal) or grain terminals (Mańkowska, Pluciński & Kotowska, 2021).

No detailed study concerning the physical properties of RSM and its separate granulometric fractions has been reported hitherto. The studies on the physical properties of individual fractions, differing in terms of particle size, have both theoretical and practical importance, especially due to the phenomenon of the natural self-sorting of rapeseed biomass in transshipment processes. A fractionation of RSM, which is primarily used as a feed component and is aimed at improving its nutritional value through the removal of larger particles (Hansen et al., 2017), has not been applied so far on an industrial scale, mainly because of the problems with the utilization of fractions with a lower feeding value. However, there is a possibility to use these coarse fractions of RSM (instead of all the material in unfractionated form, as has been practiced so far) as an alternative energy source, both in raw form (direct combustion) and after conversion to biochar (Özçimen & Karaosmanoğlu, 2004; Ucar & Ozkan, 2008). Having still considered the increasing production of bioenergy from agricultural waste in Northern European countries (Stolarski et al., 2020), fractionation of RSM becomes more economically justified, at least until yellow-seeded rapeseed lines are to be cultivated on an industrial scale (Święch et al., 2016).

This work aims to determine the selected physical properties of natural RSM and its fractions, which have an importance in the handling, storage, and transportation processes, such as true density, bulk density, angle of repose, and porosity, as well as to estimate the correlations between the physical quantities and the average particle size, accounting for the morphological diversity of separate granulometric fractions.

Material and methods

Material and separate fractions preparation

The research material was post-extracted RSM produced by ADM Szamotuły from seeds of double-low varieties (*Brassica napus* L. *var. napus*), exported by sea and handled in one of the Polish seaports (Szczecin). Fractionation of the RSM, in order to establish the particle size distribution, was performed by screening on sieves (Multiserw Morek) according to ISO 2591-1:1988. The distribution parameters were determined based on the Rosin-Rammler-Sperling-Bennet (RRSB) equation (Gupta & Yan, 2006). The equivalent diameter of particles contained in each fraction (x) was calculated as the geometric mean of marginal particle sizes (sieve mesh sizes) in accordance with Polish standard PN-R-64798:2009. The equivalent diameters for the fractions with particle size > 3 mm and < 0.075 mm were found by additional separation into sub-fractions (i). The average particle size was established using equivalent diameters of each i-fraction and their mass proportion, where the mass share of i-fraction was employed as a coefficient of weight. For the purpose of testing the characteristics of individual fractions, requiring a certain volume of samples, about 150 kg of RSM was screened, from which 750 g of dust with particle size < 0.075 mm was obtained. To separate enough of the finest dust, the time of vibration of a single sample (200 g) on the apparatus was extended above the standard used in the determination of the particle size distribution.

Chemical analysis

The chemical composition of RSM and its fractions was determined by a near-infrared spectroscopy (NIRS) method on a spectrometric FT-NIR MPA – Multi Purpose Analyzer, Bruker. The camera was equipped with an integrating sphere for loose, heterogeneous products. Samples were scanned 32 times. Quantitative results related to the selected components, corresponding to the absorbance spectra obtained, were calculated in the OPUS 6.0 program using the RSM calibration model provided by the camera manufacturer. The results were expressed as grams of the component per 100 g of dry basis (d.b.), except the moisture where the unit per wet basis (w.b.) was used.

Physical properties measurements

Microscopic tests were performed using the microscopes: Studar PZO Warszawa, with the MNP1 projection attachment made by PZO and the metallographic microscope Neophot 2, C. Zeiss. The water activity of the meal and its fractions were determined by the static method, which involves the measurements of sorption of water vapor at $t = 25°C$ and at a relative humidity of 45%, 60%, and 75%. Samples of 5 g were kept in Petri dishes in a climatic chamber type 60 U Mytron until its constant weight was achieved. The true (particle) density was determined by measuring the volume of the sample of known mass through the progressive replenishment of the flask with a liquid (i.e., ethyl alcohol). The bulk (loose) density measurements (except the finest fraction) were carried out followed PN-EN 1236:1999, using the container of 1000 cm^3 volume. The bulk density of the dust having a particle size smaller than 0.075 mm was determined in accordance with EN 50281-2-1:1999. The porosity of the meal and its fractions were calculated via the following formula:

$$\varepsilon = (\rho_t - \rho_b)/\rho_t \cdot 100\% \,, \quad (1)$$

where ε represents the porosity (%), ρ_t signifies the true density ($g{\cdot}cm^{-3}$), and ρ_b is the bulk density ($g{\cdot}cm^{-3}$).

The two methods for determination of the angle of repose were applied. The static angle of repose (AoR_s) was measured using the piling method in accordance with BN-87/91350-10 standard. The method embraces measurement of the height of the cone formed from material on a circular disk of a given diameter ($d = 120$ mm) by slowly pouring the sample from the funnel onto this base. The angle of repose was also found by the "tilting box-test" method in accordance with the IMSBC Code (IMSBC, 2018). The obtained parameter (AoR_T) is an angle formed between the horizontal and the top surfaces of the test box, when the material in the box just begins to slide in bulk. The box was tilted without shocks using a hydraulic cylinder, and the compressed air traveled at a speed of about 0.3° s^{-1}. The dimensions of the measuring instrument used, and its construction, corresponded to the requirements specified in the IMSBC Code. Due to an insufficient amount of dust with a particle size < 0.075 mm, results for this fraction were made by putting in a proper box (with internal dimensions of 400×600×200 mm) a steel container with dimensions of 250×250×80 mm. The tests for all the fractions were made at a material layer thickness of 25 mm.

Statistical analysis

The tests were carried out in six replications ($n = 6$), except for the measurements of true density for dust with particle size < 0.075 mm ($n = 3$). The statistical analysis was conducted using Statistica software (V.8.0, Statsoft Polska). The significance of differences between the mean values of measured properties for the individual RSM fractions was tested using an analysis of variance in the ANOVA module. The comparisons of means were made using the Tuckey method (post-hoc). The selection of equations describing the correlation between the empirical values of physical properties and average particle size $y = f(x)$ and further estimation of its parameters were performed in the "nonlinear estimation" module using the Lavenberg-Marquardt regression method. All structural parameters of the mathematical expressions were statistically significant at the level of $\alpha = 0.05$. The fitting of equations to experimental data was evaluated by applying the coefficient of determination (R^2) and the standard deviation of the model residues (S_e).

Results and discussion

Particle size distribution and chemical composition

The statistical average of the linear dimensions of all particles (2.2 mm), calculated by the RRSB equation ($r = 0.92$), indicates that RSM is comparable to soybean meal with regard to size distribution. The distribution parameter n amounted to 1.867 and was slightly higher than that calculated for soybean meal or oat flakes and much lower than that reached for the relatively homogeneous products including, for example, crystal sugar (Horabik & Molenda, 2002). The powdery fractions ($d < 0.4$ mm) content in examined RSM reached 24.8% by weight, while the agglomerates ($d > 1.2$ mm) content is as much as 18.3% (Table 1). The particles with a size smaller than 1 mm and those smaller than 0.65 mm reached about 75% and 50% by RSM mass, respectively. Those with a size greater than 10 mm occurred at a mass share of about 3%.

The chemical composition tests confirmed the statistically significant ($p \leq 0.05$) differentiation of the separate fractions caused by seed morphology (Table 1). The largest differences were found between the fractions with a high proportion of hulls (0.4–1.2 mm) and dust fractions (especially 0.075–0.2 mm). In extremely varied pairs of the fractions, quantitative differentiation reached 9.23 g, 4.04 g, and 5.79 g per 100 g d.m., respectively, for protein, fat, and fiber content. The consequence of varied chemical composition is a statistically significant ($p \leq 0.05$) difference in moisture content between separate fractions. The water content decreases from

Table 1. Physico-chemical characteristics of RSM and its separate granulometric fractions

Fraction (particle size) (mm)	Water activity	Moisture (% w.b.)		Crude protein (% d.b.)		Crude fiber (% d.b.)		Crude fat (% d.b.)		Fraction (%, mass)	
		Mean	SD	Mean	SD	Mean	SD	Mean	SD	Mean	SD
> 3	0.69	10.86[a]	0.22	37.71[ab]	0.46	11.48[a]	0.40	3.63[a]	0.44	12.0	1.03
1.2–3.0	0.63	9.50[b]	0.21	38.17[a]	0.88	11.79[a]	0.28	4.77[b]	0.38	6.3	0.4
0.4–1.2	0.65	10.02[c]	0.13	34.20[c]	0.56	13.66[b]	0.60	7.38[e]	0.39	56.9	1.21
0.2–0.4	0.63	9.15[d]	0.14	40.55[d]	0.36	9.37[c]	0.29	5.64[c]	0.21	18.9	0.95
0.075–0.2	0.53	7.65[e]	0.20	43.43[f]	0.24	7.87[d]	0.26	5.11[bc]	0.26	5.8	0.43
< 0.075	0.71	7.74[e]	0.15	38.47[a]	0.34	9.83[c]	0.26	3.34[a]	0.22	0.1	0.05
RSM	0.66	10.04[c]	0.19	37.03[b]	0.35	11.76[a]	0.30	6.33[f]	0.30	100	–

[a] Various letters in the same column denote significant differences in means, $n = 6$, and $p \leq 0.05$.

10% to 7.65% for the decline of the average particle size in the 1.2–0.075 mm range. The physical properties of plant-origin granular materials vary significantly, for example, with moisture content (Molenda et al., 2004; Iqbal & Fitzpatrick, 2006). However, a similar degree of water binding in these fractions was found; the water activity of the examined samples amounted between 0.53–0.71, so it was within the range of multilayer adsorption.

Density and porosity

The true density of RSM was higher (Table 2) than the values quoted in the literature for rapeseeds, i.e., 1.071–1.091 g·cm^{-3} (Unal, Sincik & Izli, 2009), since the oil removal creates a lower density. Despite the higher true density, the meal was characterized by a lower bulk density (0.538 g·cm^{-3}) in relation to data for seeds, i.e., 0.585–0.612 g·cm^{-3} (Çalişir et al., 2005). Such a dependence may be associated with particle shapes. The sphericity and roundness of the particles, being the residues after crushing, diverge from values obtained for the whole seeds, which is the reason that the porosity of meals exceeds the typical values for the spherical particle deposits. The porosity of perfectly spherical particles set varies between 26–47% (Koch & Noworyta, 2003), in some cases (e.g., soybean) it may even drop below 23% (Kibar & Öztürk, 2008); for various rapeseed cultivars, it ranges between 36.6% and 41% (Unal, Sincik & Izli, 2009). The average porosity of the examined RSM (58.4%) is similar to those reported by Horabik and Molenda (Horabik & Molenda, 2002) for maize (60%) or soya (63%) meals. The varied share of the finest particles and moisture content has an influence on a wide range of bulk density values measured in oily meals in practice (Kukelko et al., 1988; Fürll & Hoffmann, 2013).

Statistical differences ($p \leq 0.05$), in the true and bulk densities, between the fractions of the meal were noticed. The true density decreases as the average particle size increases, but only up to 3 mm. As the particles present in the coarse fraction (at the range above 3 mm) are solely lumps, the correlation between the true density and the average particle size was calculated but excluded the above fraction. The optimal matching to the empirical data

Table 2. Physical properties of RSM and its separate granulometric fractions

Fraction (particle size) (mm)	True (particle) density (g·cm^{-3})		Bulk (loose) density (g·cm^{-3})		Porosity (%)		AoRs (deg)		AoR$_T$ (deg)	
	Mean	SD	Mean	SD	Mean	SD	Mean	SD	Mean	SD
> 3	1.317[a]	0.011	0.528[a]	0.002	59.9[a]	0.37	30.69[a]	0.98	36.00[a]	0.55
1.2–3.0	1.258[b]	0.005	0.499[b]	0.002	60.3[a]	0.17	29.92[a]	0.30	33.08[b]	0.58
0.4–1.2	1.292[c]	0.011	0.469[c]	0.002	63.7[b]	0.29	30.72[a]	0.36	33.42[b]	0.58
0.2–0.4	1.327[ad]	0.011	0.557[d]	0.001	58.0[c]	0.34	33.37[b]	1.32	35.58[a]	0.49
0.075–0.2	1.342[d]	0.008	0.563[d]	0.001	58.1[c]	0.23	38.27[c]	0.97	41.25[c]	0.52
< 0.075	1.368[e]	0.013	0.490[b]	0.013	64.2[b]	0.35	49.57[d]	0.56	59.42[d]	0.38
RSM	1.292	0.013	0.538	0.002	58.4	1.82	35.81	0.36	38.40	0.75

[a] Various letters in the same column denote significant differences in means, $n = 6$, and $p \leq 0.05$.

was obtained by describing the relationship between the true density and particle size with an exponential function (R^2 = 0.93; S_e = 0.0129); this is shown in Figure 1, where y is the estimated value of true density (g·cm^{-3}) and x is the equivalent diameter of particles (mm). The true density of particle sets increases when the average particle size decreases, which is due to the diminishing share of the seed coats in separate fractions.

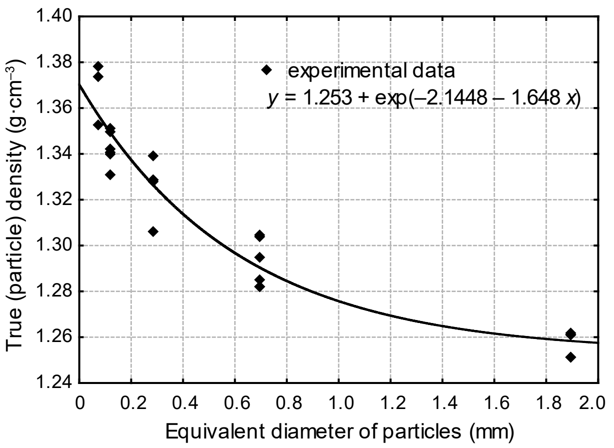

Figure 1. Relationship between the average particle size and true density of RSM fractions

No correlation was observed between the average particle size and the bulk density. In spite of the high true density, the smallest dust (d < 0.075 mm) featured a low bulk density, statistically different even when compared to dust with a slightly larger particle size (0.075–0.2 mm). During the process of pouring from the top the finest dust, the formulation of empty spaces between the groups of agglomerated particles was observed. It is commonly known that more cohesive powders have greater surface attractive forces, which help them overcome gravity; therefore, those particles can support themselves around void spaces (Fitzpatrick, 2013). The bulk density variability depends only on 23% of the true density (r = 0.48). The clusters of points in Figure 2, corresponding to individual fractions, confirm the stronger influence on the bulk density of other particle properties affected by their mutual arrangement in deposit, such as dimensions, shape, surface roughness, water content, or cohesion forces.

The relatively high porosity of the 0.4–1.2 mm fraction in comparison with the dust having a particle size in the range of 0.2–0.4 mm (63.7% vs 58%) seems to be an unexpected result, considering its high degree of polydispersity. A specific surface structure of the hull's particles appears to be of importance for this form of porosity variation since fragments of the shell are characterized by numerous cavities (Figure 3b). Such a structure is related to a palisade seed layer made of cells, between which there are free spaces with a thickness of 30 µm. Various sculptured surfaces of the seed coats with a high degree of pores and cavities were reported for other species as well (Gabr, 2014). A higher porosity of fraction 0.4–1.2 mm may, therefore, be associated

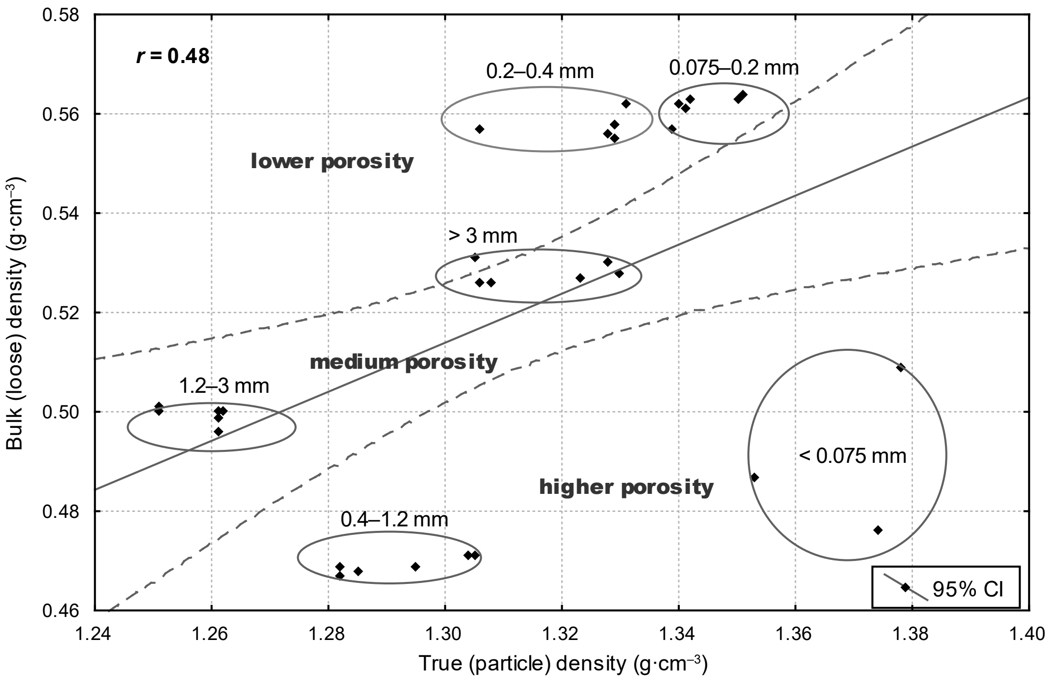

Figure 2. Relationship between the true (particle) density and bulk (loose) density of the RSM fractions

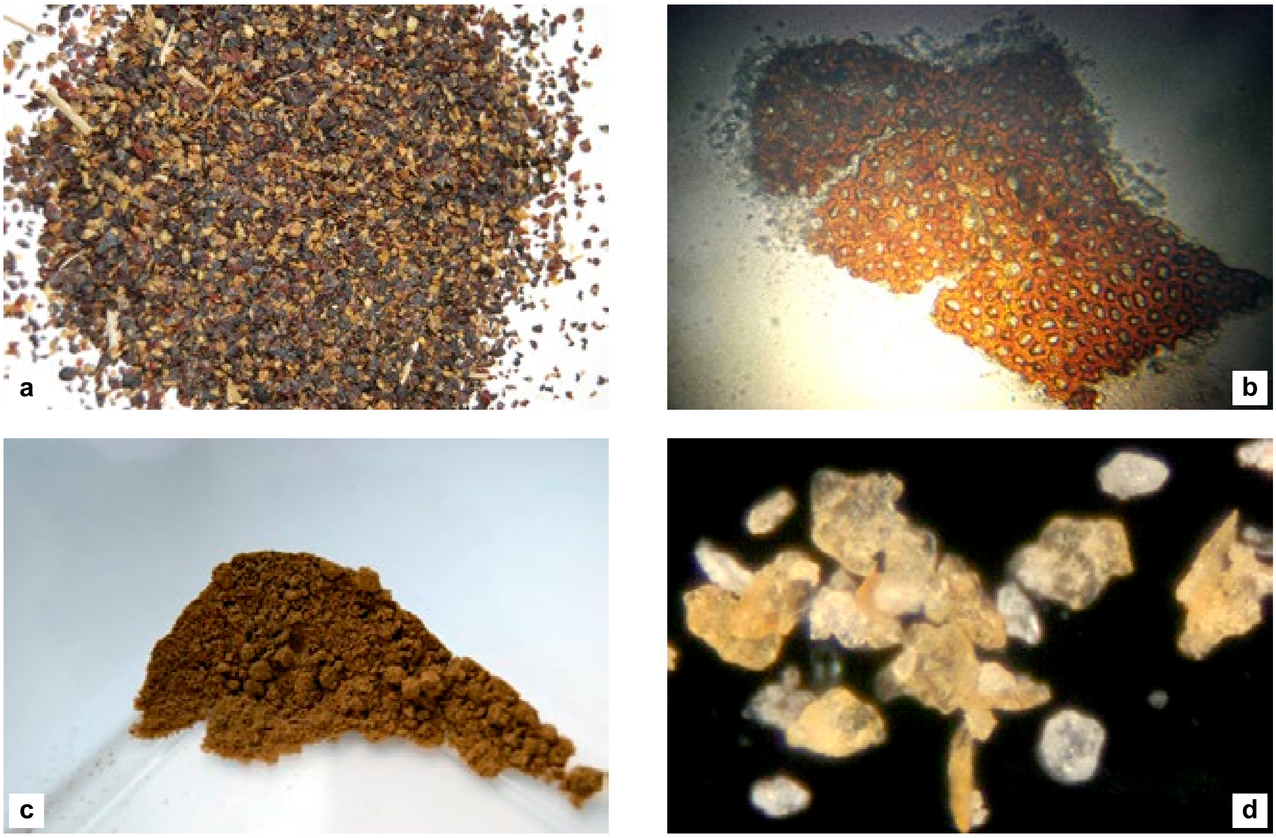

Figure 3. Exemplary particles of RSM with different morphological origins: (a) quantitative proportion of cotyledon and seed coat fragments (dark particles) in fraction 0.4–1.2 mm, (b) seed coats with a visible shape for the flake and porous structure (×160), (c) complexes of particles in fraction with particle size < 0.075 mm, and (d) cotyledon fragments in adhesive complexes in fraction with particle size < 0.075 mm

with the morphological features of the particles, not with their mutual arrangement in the deposit.

Specific physical properties of the separate fractions

Macro- and micro-scopic examinations showed differentiation in the shape and dimensions of RSM particles. The two most coarse fractions ($d > 1.2$ mm) contained the majority of the agglomerates with the shape approaching spheroid. In the fraction with a particle size of 0.4–1.2 mm, seed coat shreds prevailed quantitatively (Figure 3a). The characteristic feature of seed coat residues (remaining on a sieve with a mesh size of 0.4 mm) is their shape of flake, resulting from two large dimensions of the particles compared to the third one being the natural thickness of the rapeseed hulls. The shapes of the particles contained in the medium dusty fractions (0.2–0.4 mm and 0.075–0.2 mm) turned out to be very irregular. In the finest dust ($d < 0.075$ mm), observations on a macroscopic scale showed the presence of agglomerated clusters of particles that were easily separated by vibration (Figure 3c). Additionally, the microscopic images showed numerous complexes of more strongly adherent particles having maximum linear dimensions up to 0.2 mm that were not easily separated (Figure 3d), which is in opposition to clusters on a macro-scale. It has been accepted that particles that have a size below a certain threshold (usually 0.1–0.5 mm) become cohesive, and those smaller than 0.01 mm are extremely cohesive (Horabik & Molenda, 2002; Liu et al., 2008). In the case of fine powders, the inter-particle force becomes dominant, which causes the phenomena of particles behaving not as individuals but as cohesive groups (Wang et al., 2010).

Angle of repose

According to Carr's classification (Beakawi Al-Hashemi & Baghabra Al-Amoudi, 2018), unfractionated RSM can be treated as a material acting between those that are free-flowing (30–38°) and "fair to passable flowing" (38–45°). Similar results were presented by Kukelko et al. (Kukelko et al., 1988) for canola meals. The dusty fractions were characterized by statistically significant ($p \leq 0.05$) differentiation in terms of AoR, but no significant differences were found in the case of coarse fractions. Along with a decrease in the average particle size from 0.4 mm, an increase in the AoR_T and AoR_S was found. It was established that the dependences of these angles (where y is the estimated values of AoR_s and AoR_T) on the equivalent diameter of particles (x) are exponential ($R^2 = 0.96$; $S_e = 1.303$ for AoR_s/$R^2 = 0.98$, $S_e = 1.151$ for AoR_T). Experimental data with estimation formulas are presented in Figures 4 and 5.

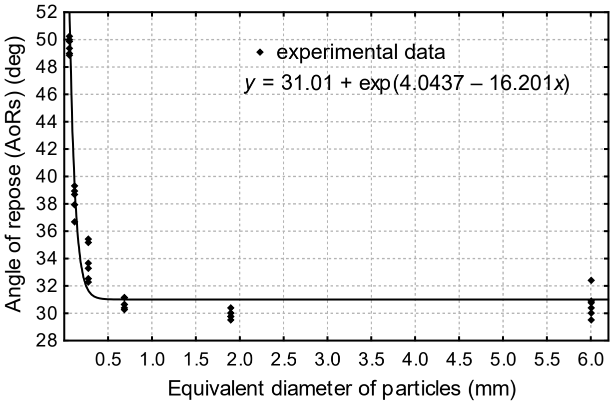

Figure 4. Relationship between the average particle size and AoR_s of RSM fractions

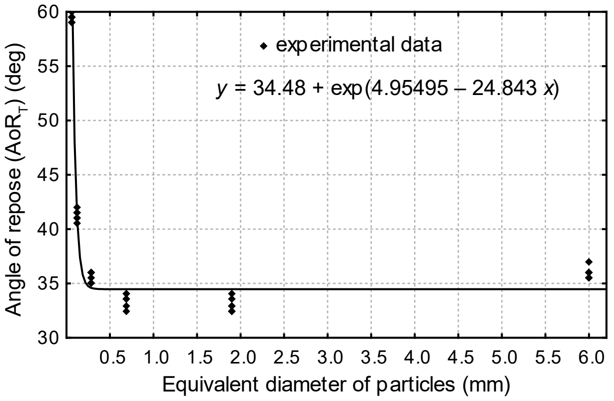

Figure 5. Relationship between the average particle size and AoR_T of RSM fractions

Higher AoR measured for the unfractionated RSM (35°and 38°), compared to the values obtained for separate fractions (except the two finest dust fractions), seems to be determined by the particle size polydispersity and the geometric diversity, which jointly contribute to the mutual interlockings. When the particles are set up with size and shape polydispersity, according to results given by Mattutis et al. (Mattutis, Luding & Herrmann, 2000) in model experiments, the static angle of repose measured on the pile depends equally on shape, range of fluctuations from the monodispersity, and the heap's construction history. In the fraction with a particle size of 0.4–1.2 mm, the reason for the relatively low AoR may be the flaked shape of the shells. Accounting for over a 50% quantitatively share of the hull residues in this fraction, it may be deduced that those sets of particles would slide on their flat surfaces rather than roll. This tendency to either roll or slide is very important because most flat materials slide easier than spherical ones (Coşkuner & Gökbudak, 2016). Similarly, the most coarse sets of particles ($d > 3$ mm and 1.2–3 mm) featured a tendency to be free-flowing, which was expected regarding the observed shape of the granules and their smooth texture. It has been proven by other studies that angular particles interlock more thoroughly than rounded ones; therefore, generally, the more spherical the particles, the smaller the angle of repose (Matuttis, Luding & Herrmann, 2000; Shinohara, Oida & Golman, 2000; Khanal, Elmouttie & Adhikary, 2017).

The flowability of the granular materials is affected, for example, by the size distribution, but there were reports in the literature of critical particle size, below which the effect of that factor is reversed (Liu et al., 2008). It was observed that, only in the case of larger particles, the smaller the differentiation in particle size, the greater the flowability (i.e., a smaller AoR). Such a correlation is not so obvious in the case of powders. While a high AoR obtained for the natural meal (compared to values for individual coarse fractions) can be explained by its polydispersity and heterogeneity, the reverse phenomenon occurs in the case of fine dust. According to the results of other authors (Liu et al., 2008), below a certain critical size, the monodispersity reduces the flowability, which may be a partial explanation for the observed AoR rapid increase with the average particle size decreasing from the size of 0.2 mm (Figures 4 and 5). The mutual homogeneity of the surface of such dust may be of great importance as well, as reported by Horabik and Molenda (Horabik & Molenda, 2002); namely, the fastest increase in the coefficient of friction occurs when the unevenness of the rubbing surface approaches the unevenness of the granular material surface. The above is consistent with the obtained results since the interactions of morphologically homogeneous dust particles ($d < 0.2$ mm) concern surfaces of the same unevenness. Not without significance for the observed high values of AoR, for the finest fractions ($d < 0.2$ mm), it may also be a greater cohesion of particles, increasing with the degree of fragmentation. For dry powders, these cohesion forces can be classified as van der Waals, electrostatic, and magnetic (Fitzpatrick, 2013). The smaller the particle size, the greater the contact surface area per unit mass of powder and, thus, the greater van der Waals attractions between the particles.

Manikantan et al. (Manikantan, Ambrose & Alavi, 2015) stated that the cohesive behavior of coconut flour depends on the particle size, moisture content, and chemical composition, especially on protein and fat concentrations due to their contribution to agglomeration. Among the above factors, in studied RSM, only particle size and residual oil seem to have any importance in relation to the increasing cohesion, which is reflected by a vast difference in the AoR_S and AoR_T (over 11 and 18 degrees, respectively) between the two tiniest fractions (0.075–0.2 mm and $d < 0.075$ mm). The visible particle complexes on the micro- and macro-scale were observed exclusively for the finest dust, despite the higher protein content for the fraction 0.075–0.2 mm (43.4% vs. 38.5%) and comparable moisture content (Table 1). The increase in the coefficient of friction seems not to be a reason for that phenomenon because, morphologically, the surfaces of these two dust fractions did not differ.

Based on the previous observations, and the research carried out in this work, it is possible to formulate good operational practices, including systematic removal of dust layers from surfaces of transportation means and other devices, as well as reducing dust-air mixture formations during all handling operations. Considering the necessity to prevent dust auto-ignition and explosion, this should be standard practice when handling any plant-derived dusty material. The obtained results indicate an additional positive aspect of such treatments, i.e., an increase in the flowability of RSM. Only in the case of sea transport is the low flowability of RSM a desirable feature since it means its relatively low susceptibility to shift into the sides of the ship during a journey. According to the IMSBC Code, cargoes with an angle of repose above 35^0 are considered relatively safe in this aspect, which indicates the least restrictive rules for their trimming (IMSBC, 2018). In railway and road transport, especially in reloading processes as well as during handling in storage chambers, low flowability of RSM causes difficulties in ensuring the correct and safe course of these operations.

Elimination of the phenomena of self-sorting during the loading of storage tanks, chambers, silos, and land means of transport is practically not possible with typically used technologies. The exception here is ships and barges, where a solution to prevent segregation by particle size is a handling carried out in holds (trimming) and the changing position of the loading devices in the horizontal plane. Self-sorting, i.e., stratification of the bulk granular mass as a result of varied density or particle size, causes an uneven distribution of particles in the storage space (Bowszys, 2007). Particles with higher true density or larger particle sizes fall faster and accumulate at the bottom of the tank, while those that are lighter or finer are concentrated at the tank walls. During unloading, the heavier and/or coarser material flows out first, followed by contaminants and fine dust particles. Considering the various physical properties of the RSM separate fractions, the construction of the bottom parts of tanks, bins, hoppers, and transfer chutes should be adapted to the most problematic fraction (namely, the dusty ones) in order to avoid problems with material blockage during unloading. One of the solutions for adapting existing infrastructure may be the use of non-adhesive linings, which prevent or significantly reduce the sticking of stored material in hoppers and chamber chutes. An additional option is the installation of aeration nozzle systems or air cannons in the outlets of the silos, which eliminate the bridging of the load during unloading. Results of experimental research confirmed the principles of good practice, i.e., RSM biomass should not be stored in universal silos, especially those not equipped with additional protection against implosion, neither in those with outlets designed for very flowing (AoR < 30°) and free-flowing (30° < AoR < 38°) materials. Recommended storage building for this type of material is a flat-bottomed warehouse where the load is held in the form of a heap.

Conclusions

Geometrically and chemically varied residues of seed coats and cotyledons make RSM a heterogeneous material. The physical properties of the separate granulometric fractions of RSM, important in storage, handling, and transportation processes, depend on the particle size as well as their morphological origin that affects the varied chemical composition, water content, shape (roundness and sphericity), and texture of the particles (roughness and pores). The smallest dust fractions ($d < 0.075$ and 0.075–0.2 mm) are composed exclusively of cotyledons, which causes a vast discrepancy in the particle density, bulk density, porosity, and angles of repose (static and dynamic) between the dusty fractions and those that are coarser, as well as between each other. The inherent properties of the particulate materials, such as cohesion and adhesion, as well as the homogeneity of dust particles, have an impact on the variation of these properties between dust fractions due to the absence of seed coats.

It can be concluded that a relatively low tendency to free flowing of RSM is mainly caused by its wide-ranging particle size distribution and geometry differentiation, which facilitates mutual particle interlockings. This interpretation was supported by the results obtained for individual fractions – each of the four coarse fractions showed separately much greater flowability than the natural meal. Only dust with a particle size less than 0.2 mm had a significantly lower flowability and, therefore, may be responsible for the known cases of blockages of silos, bins, hoppers, and transfer chutes.

The research carried out in the present work should enable a formulation of general recommendations in the field of handling, transportation, and storage processes of RSM biomass. Accounting for the specific properties of this cargo, its logistics service should be carried out only with the use of specialized infrastructure, and, moreover, it would be advisable to specify physical properties in each new by-product obtained from the rapeseed. Failure to comply with the above conditions may result in problems with ensuring the continuity of the logistics chain, and, in extreme cases, it could lead to serious consequences that include the implosion of the silo.

References

1. Beakawi Al-Hashemi, H.M. & Baghabra Al-Amoudi, O.S. (2018) A review on the angle of repose of granular materials. *Powder Technology* 330, pp. 397–417.
2. BN-87/91350-10. Pasze prasowane. Oznaczanie kata naturalnego usypu granul i brykietów.
3. Bojanowska, M., Chmiel, J. & Pańcyk, K. (2016) The role of dust fractions of rapeseed meal in the wear of cargo handling system. *Solid State Phenomena* 252, pp. 21–30.
4. Bojanowska, M. & Leśmian-Kordas, R. (2009) Wybuchowość pyłów śruty rzepakowej. *Polish Journal of Commodity Science* 1, pp. 102–115.
5. Bowszys, J. (2007) Rozwarstwianie nasion rzepaku podczas wypływu z silosów. *Inżynieria Rolnicza* 9 (97), pp. 21–26.
6. Çalişir, S., Marakoğlu, T., Öğüt, H. & Öztürk, Ö. (2005) Physical properties of rapeseed (*Brassica napus oleifera* L.). *Journal of Food Engineering* 69, pp. 61–66.
7. Carr, M.J., Roberts, A.W. & Wheeler, C.A. (2019) A revised methodology for the determination of bulk material cohesion and adhesion. *Advanced Powder Technology* 30, pp. 2110–2116.
8. Chibowska, M., Smulikowska, S. & Pastuszewska, B. (2000) Metabolizable energy value of rapeseed meal and its fractions for chickens as affected by oil and fibre content. *Journal of Animal and Feed Sciences* 9, pp. 371–378.
9. Coşkuner, Y. & Gökbudak, A. (2016) Dimensional specific physical properties of fan palm fruits, seeds and seed coats (*Washingtonia robusta*). *International Agrophysics* 30, pp. 301–309.
10. EN 50281-2-1:1999. Electrical apparatus for use in the presence of combustible dust. Part 2–1: Test methods. Methods of determining minimum ignition temperatures of dust.
11. Fauduet, H., Coic, J.P., Lessire, M., Quinsac, A., Ribaillier, D. & Rollin, P. (1995) Rapeseed meal upgrading – pilot scale preparation of rapeseed meal materials with high or low glucosinolate contents. *Animal Feed Science and Technology* 56, pp. 99–109.
12. Fediol (2021) *Evolution 1980–2021.* [Online] Available from: https://www.fediol.eu/web/evolution%201980%20%202018/1011306087/list1187970169/f1.html [Accessed: September 01, 2021].
13. Fitzpatrick, J. (2013) Powder properties in food production systems. In: Bhandari, B., Bansal, N., Zhang, M. & Schuck, P. (Eds). *Handbook of food powders. Processes and properties*. UK: Woodhead Publishing Limited.
14. Fürll, C. & Hoffmann, T. (2013) Flow properties of components for dry compound feed. *Powder Technology* 235, pp. 838–841.
15. Gabr, D.G. (2014) Seed morphology and seed coat anatomy of some species of Apocynaceae and Asclepiadaceae. *Annals of Agricultural Science* 59, pp. 229–238.
16. Gupta, A. & Yan, D. (2006) *Mineral Processing Design and Operation. Chapter 2. Particle Size Estimation and Distributions*. Elsevier Science.
17. Hansen, J.Ø., Skrede, A., Mydland, L.T. & Øverland, M. (2017) Fractionation of rapeseed meal by milling, sieving and air classification – Effect on crude protein, amino acids and fiber content and digestibility. *Animal Feed Science and Technology* 230, pp. 143–153.
18. Horabik, J. (2001) *Charakterystyka właściwości fizycznych roślinnych materiałów sypkich istotnych w procesach składowania*. Acta Agrophysica 54. Lublin: Institute of Agrophysics, Polish Academy of Sciences.
19. Horabik, J. & Molenda, M. (2002) *Właściwości fizyczne sypkich surowców spożywczych.* Acta Agrophysica 74. Lublin: Institute of Agrophysics, Polish Academy of Sciences.
20. IMSBC (2018) International Maritime Solid Bulk Cargoes Code and Supplement, IMO, London.
21. Iqbal, T. & Fitzpatrick, J.J. (2006) Effect of storage conditions on the wall friction characteristics of three food powders. *Journal of Food Engineering* 72, pp. 273–280.
22. ISO 2591-1:1988. Test sieving – Part 1: Methods using test sieves of woven wire cloth and perforated metal plate.
23. Khanal, M., Elmouttie, M. & Adhikary, D. (2017) Effects of particle shapes to achieve angle of repose and force displacement behavior on granular assembly. *Advanced Powder Technology* 28, pp. 1972–1976.
24. Kibar, H. & Öztürk, T. (2008) Physical and mechanical properties of soybean. *International Agrophysics* 22, pp. 239–244.
25. Koch, R. & Noworyta, A. (2003) *Procesy mechaniczne w inżynierii chemicznej*. 3rd Edition Warszawa: WNT.
26. Kukelko, D., Jayas, D.S., White, N.D.G. & Britton, M.G. (1988) Physical properties of canola (rapeseed) meal. *Canadian Agricultural Engineering* 30, pp. 61–64.
27. Liu, L.X., Marziano, I., Bentham, A.C., Litster, J.D., White, E.T. & Howes, T. (2008) Effect of particle properties on the flowability of ibuprofen powders. *International Journal of Pharmaceutics* 362, pp. 109–117.
28. Manikantan, M.R., Ambrose, R.P.K. & Alavi, S. (2015) Flow specific properties of coconut flours. *International Agrophysics* 29, pp. 459–465.

29. Mańkowska, M., Pluciński, M. & Kotowska, I. (2021) Biomass sea-based supply chains and the secondary ports in the era of decarbonization. *Energies* 14, 1796.
30. Matuttis, H.G., Luding, S. & Herrmann, H.J. (2000) Discrete element simulations of dense packings and heaps made of spherical and non-spherical particles. *Powder Technology* 109, pp. 278–292.
31. Mińkowski, K. (2002) Influence of dehulling of rape seeds on chemical composition of meal. *Animal Feed Science and Technology* 96, pp. 237–244.
32. Molenda, M., Horabik, J., Thompson, S.A & Ross I.J. (2004) Effects of grain properties on loads in model silo. *International Agrophysics* 18, pp. 329–332.
33. Özçimen, D. & Karaosmanoğlu, F. (2004) Production and characterization of bio-oil and biochar from rapeseed cake. *Renewable Energy* 29, pp. 779–787.
34. PIP (2006) Państwowa Inspekcja Pracy Oddział Opole, Ślósarczyk, J. & Warsitz, M. Implozje w silosach. *Inspektor Pracy* 4, pp. 21–23.
35. PN-EN 1236:1999. Nawozy – Oznaczanie gęstości nasypowej (luźnej).
36. PN-R-64798:2009. Pasze – Oznaczanie rozdrobnienia.
37. Shinohara, K., Oida, M. & Golman, B. (2000) Effect of particle shape on angle of internal friction by triaxial compression test. *Powder Technology* 107, pp. 131–136.
38. Sosulski, F. & Zadernowski, R. (1981) Fractionation of rapeseed meal into flour and hull components. *Journal of the American Oil Chemists' Society* 58, pp. 96–98.
39. Stolarski, M.J., Warmiński, K., Krzyżaniak, M., Olba-Zięty, E. & Akincza, M. (2020) Bioenergy technologies and biomass potential vary in Northern European countries. *Renewable and Sustainable Energy Reviews* 133, 110238.
40. Sturaro, A., Rella, R., Parvoli, G., Ferrara, D. & Doretti, L. (2003) Chemical evidence and risks associated with soybean and rapeseed meal fermentation. *Chemosphere* 52, pp. 1259–1262.
41. Święch, E., Raj, S., Pastuszewska, B., Taciak, M., Bartkowiak-Broda, I. & Smulikowska, S. (2016) Nutritional value of yellow-seeded winter rapeseed cakes for growing pigs. *Agricultural and Food Science* 25, pp. 99–110.
42. Ucar, S. & Ozkan, A.R. (2008) Characterization of products from the pyrolysis of rapeseed oil cake. *Bioresource Technology* 99, pp. 8771–8776.
43. Unal, H., Sincik, M. & Izli, N.C. (2009) Comparison of some engineering properties of rapeseed cultivars. *Industrial Crops and Products* 30, pp. 131–136.
44. USDA (2022) United States Department of Agriculture Foreign Agricultural Service. *Oilseeds: World Markets and Trade*. Available from: https://www.fas.usda.gov/data/oilseeds-world-markets-and-trade [Accessed: October 17, 2022].
45. Wang, W., Zhang, J., Yang, S., Zhang, H., Yang, H. & Yue, G. (2010) Experimental study on the angle of repose of pulverized coal. *Particuology* 8, pp. 482–485.

Cite as: Bojanowska, M. (2023) Handling and transportation properties of rapeseed biomass as affected by particle size. *Scientific Journals of the Maritime University of Szczecin, Zeszyty Naukowe Akademii Morskiej w Szczecinie* 74 (146), 5–15.